Metallurgy and materials
Metalurgia e materiais

Steel desulfurization on RH degasser: physical and mathematical modeling

http://dx.doi.org/10.1590/0370-44672021750058

Antonio Marlon Barros Silva[1,2,4]
https://orcid.org/0000-0003-0414-2893
Johne Jesus Mol Peixoto[3,5]
https://orcid.org/0000-0002-1648-5423
Carlos Antônio da Silva[3,6]
https://orcid.org/0000-0002-2100-9149
Itavahn Alves Silva[3,7]
https://orcid.org/0000-0002-7048-7163

[1]Universidade Federal de Ouro Preto -UFOP, Escola de Minas, REDEMAT - Rede Temática em Engenharia de Materiais, Ouro Preto - Minas Gerais – Brasil.

[2]Instituto Federal de Educação, Ciência e Tecnologia de Minas Gerais - IFMG, Ouro Branco - Minas Gerais - Brasil.

[3]Universidade Federal de Ouro Preto – UFOP, Escola de Minas, Departamento de Engenharia Metalúrgica, Ouro Preto – Minas Gerais – Brasil.

E-mails: [4]antoniomarlon.silva@ifmg.edu.br, [5]johnepeix@yahoo.com.br, [6]casilva@ufop.edu.br, [7]itavahnufop@yahoo.com.br

Abstract

Due to the high-quality steel demand, especially for ultra-low Sulfur steel, RH desulfurization has been practiced. Based on this, mathematical and physical modeling have been applied to study steel desulfurization by reagent addition in the RH degasser vacuum chamber. The main result of cold modeling, using water and oil emulating steel and slag, respectively, was to assess the influence of density difference between the continuous and disperse phases on oil droplet behavior. It is shown that its flow tends to be more restricted near the down snorkel when the density difference increases. Moreover, these results provide the basis for CFD modeling validation, which enabled the determination of slag drop residence time inside steel on RH and the average value of the rate of dissipation of turbulent kinetic energy inside the RH ladle. These two parameters were used to develop a kinetic model, which reaches a good agreement with industrial trial results available in literature. The optimum desulfurization degree of 31.44% was achieved for a gas flow rate of 90 Nm^3/h, according to the kinetic model. This value can be useful in some steel grade production, where the required S content is less than 10 ppm. Even in common steel grade production, if some punctual chemical adjustment is necessary, this technique is also useful. The main kinetic parameter for steel desulfurization is the steel circulation rate. For best results, it should be reduced in the desulfurization stage, and after that, the normal operation can be resumed, so that the production cycle is not affected.

Keywords: RH degasser; steel desulfurization, modeling of steelmaking.

1. Introduction

Sulfur has a deleterious effect on steel properties, demanding high desulfurization efficiency in the iron and steelmaking process. Although expressive amounts of sulfur are already removed in the blast furnace and hot metal pretreatment, for some steel grades (S <10 ppm), such as ocean, aeronautic, pipeline, plate and bearing steel, additional desulfurization

(de-S) is required (Ghosh, 2001; Peixoto *et al*., 2018).

After hot metal pretreatment, it is possible to desulphurize in the secondary refining. In the case of primary refining, oxidizing refining, de-S is not efficient (Riboud and Vasse, 1985; Torres, 2017). RH degasser is one of the reactors frequently used during secondary metallurgy and can perform desulphurization, since high basicity slags and low oxygen potential, required for steel desulphurization, can be achieved (Silva *et al*., 2021). In this reactor, a vigorous agitation, especially in the vacuum chamber, is present, resulting in a good steel desulfurization opportunity. Moreover, de-S at RH prevents N and H pick-up, which is not possible in Ca-bearing reagent injection during ladle metallurgy (Szekely *et al*., 1989; Wei *et al*., 2000).

Some steel desulfurization models, which take into consideration addition of CaO-Al_2O_3-(CaF_2) based materials in the vacuum chamber do forecast good de-S results (Van Der Knoop *et al*., 1996; Zulhan *et al*., 2013; Yang *et al*., 2014). However, some of them assume that the added slag remains in the chamber during the degassing treatment which, according to Peixoto *et al*. (2018) and Dai *et al*. (2020), using physical and numerical modeling, should not occur.

Although the thermodynamic condition at RH is favorable to Sulfur removal, it is not so from a kinetic point of view. In a few minutes after the material addition on the vacuum chamber, the desulfurizer agent is dragged to the ladle due to high turbulence, being quickly floated and absorbed by the top slag layer, which is essentially stagnant and not active for desulphurization (Dai *et al*., 2020; Yang *et al*., 2014).

For efficient desulfurization, desulfurizer material must be dispersed into the steel for enough time (high residence time). During RH degassing, by a reduction of the circulation rate, it is possible to increase the desulfurizer reagent residence time, improving desulfurization. However, this could decrease productivity, degassing capacity and increase heat losses, as cited in Yang *et al*., (2014).

There are many studies involving liquid/liquid mass transfer inside agitated gas reactors, but few for RH. Furthermore, there are still issues regarding de-S at RH, like the conditions that lead to slag entrainment and the flow of droplets dragged from the vacuum vessel to the lower vessel through the down leg. The aim of this study is to evaluate the best conditions to increase slag droplet residence time inside steel, without compromising the reactor productivity. The slag-metal behavior was investigated by physical modeling with different types of oil and aqueous solutions and numerical modeling (CFX-ANSYS), too. In addition, mass transfer tests were conducted in a cold physical model, using water, oil and thymol as steel, slag and tracer (S), respectively. The combination of all these tests and simulations allowed the development of a kinetic model for desulfurization prediction in RH.

2. Materials and methods

Experimental work was conducted in a physical model (1:7.5) built in acrylic and using oil/water to simulate steel melt/slag in the RH degassing industrial unit. Geometric and operational parameters regarding model and industrial reactor (prototype) are given in literature (Seshadri and Costa, 1986; Peixoto, 2019).

Prototype and model similarity was assured by the proper choice of three dimensionless numbers: (1) - Froude number (Fr), (2) - flow number (Nva) and (3) - modified Froude number (Frm). Details regarding similarity in RH modeling are given in Seshadri and Costa (1986), Peixoto (2019), Silva *et al*. (2021).

$$Fr = \frac{V^2}{gD} \qquad (1)$$

$$Nva = \frac{G}{VD^2} \qquad (2)$$

$$Frm = \frac{\rho_g G \left(\frac{G}{\phi^2}\right)}{\rho_l g D^3} \qquad (3)$$

Here V stands for liquid velocity, D for snorkel diameter, G for gas flow rate, ∅ is the gas injection nozzle diameter, g is the gravity acceleration, ρ_l and ρ_g are the liquid and gas densities, respectively.

2.1 Thymol mass transfer in an oil-aqueous solution system

Thymol ($C_{10}H_{14}O$) was used as a tracer element to simulate sulfur transfer from slag to steel, as suggested by Kim and Fruehan (1987) and Abreu *et al*. (2020). These authors reported a water/vegetable oil thymol partition coefficient value close to the steel-slag system, 3-4x10^2 in magnitude. Preliminary experiments, here called bench tests, in which different oils (24 mL) and a thymol aqueous solution (1.0 L, ~100 ppm thymol) were vigorously mixed in a beaker, have been performed in order to assess the partition coefficient. The methodology is fully described in Abreu *et al*. (2020) and Peixoto (2019). The partition coefficient, here defined as L_t = [thymol]oil / [thymol] water), as well as other properties of the fluids, are listed in Table 1.

For each experimental condition, thymol concentration ([thymol]) in water was measured from samples collected during the RH model operation. An UV spectrophotometer (Model S100) with MetaSpec Pro analysis software has been used, see Abreu *et al*. (2020) and Peixoto (2019) for more details.

For the mass transfer tests in the physical model, the ladle was filled with 89 L of aqueous solution (thymol concentration ~ 100 ppm). This solution was circulated for two minutes before oil addition. This is important to guarantee homogenization and flow field development. Furthermore, the RH typical and regular flow patterns are obtained.

Oil addition was made with a discharge tube positioned in the center of the vacuum chamber at 10 cm from the surface of the liquid (~ 16.5 cm from chamber bottom). The oil volume was determined according to the average consumption of desulfurizing material (10 kg/t of steel), 2 L of oil in this case.

Aqueous solution samples (~ 15 mL)

were taken at: 0; 0.5; 1; 1.5; 2; 3; 4; 5; 6; and 10 minutes, from a small tube positioned below the up-leg at 20 cm from the ladle bottom. From these measurements, the kinetic curve was fitted for three gas flow rates values: 70, 90 and 110 NL/min.

It is worthy to mention that the sample taken was filtered to retain possible oil droplets that reached the sampling tube. Every sample was placed in an Erlenmeyer, which was then capped to restrain evaporation losses.

2.2 Numerical modeling

Numerical modeling was performed with CFX - ANSYS. In order to reduce computational costs, only half of the reactor was taken into account. That is possible, since there is a symmetry plane at RH degasser, see Figure 1. The numerical model was validated using the results from physical modeling (Peixoto, 2019).

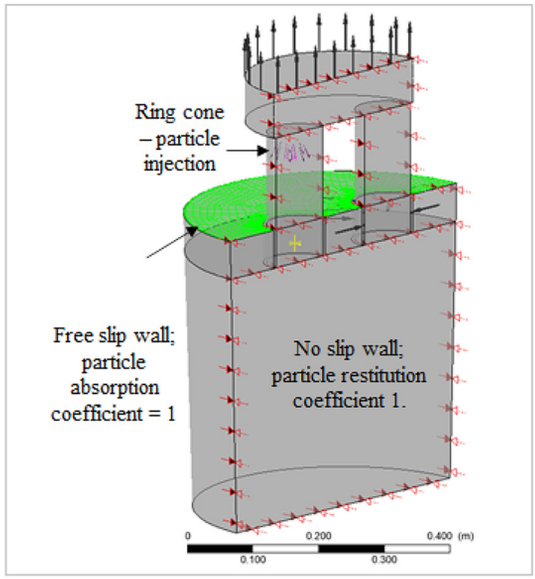

Figure 1 – Domain of numerical simulation of RH degasser.

To ensure that the mesh size used is adequate, a mesh independence study was performed by comparing the circulation rate obtained with meshes of various sizes.

With the flow pattern determined in a previous study (Peixoto, 2019), the oil particle trajectory inside the physical model and slag in the prototype were simulated in a steady state, using particle injection into a vacuum chamber. The Euler-Lagrange approach is implemented in CFX as a particle transport model. This model is suitable for describing multiphase behavior, in particularly discrete phase behavior, by tracking one or a group of particles through the continuous fluid flow using the Lagrangian description of the particle motion. The integration of the particle path through the discrete domain gives the particle trajectory (CFX-Solver Theory Guide, 2018).

Considerations for the liquid-particle interaction model: the Schiller Naumann model was chosen for drag force on the particle; the virtual mass force coefficient was equal to 0.25; particle dispersion model for turbulent dispersion force. The pressure gradient force was neglected. A fixed surface (without air layer) within the vacuum chamber has been considered. Drop injection was performed using a 30° cone inside a vacuum chamber, above and at centerline of the down leg. The software was set to calculate 100 trajectories, corresponding to 100 injection position. The drop mass flow rate at the injection point was about 10% of the average drag rate of 2L of N-pentane when the gas flow rate was 110L/min (0.1x 2Lx 0.626 kg/L ÷ 38.6 s = ~ 0.003 kg/s) in the physical model. Drop speed was set as zero slip velocity, so, the injected droplets have the same velocity of the local continuous phase. The droplet's diameter was kept constant, and no particle coalescence or break-up were considered.

The droplet size distribution was set considering the normal in diameter by mass, whereby 5 mm, 12 mm, 8 mm and 2 mm are the minimum, the mean, the maximum and the standard deviation, respectively.

Three oils were considered for modeling with a 110 L/min gas flow rate: 10W30 engine oil, N-pentane and soybean oil. Material properties are shown in Table 1.

Table 1 – Physical properties set on RH numerical model.

Material X	Density (kg/m³)	Viscosity		Interfacial tension σ (mN/m) [c]		Thymol partition coefficient[c]
		cSt [a]	mPa.s	X/air	X/water	
Water	1000	1	1	72.0	-	-
Engine oil - 10 W30	855 [c]	158.2 [c]	135.3	20.8	12.9	35.3
Soybean oil	914.3[c]	54.9[c]	52.2[c]	28.64	35.6	439.2
N-pentane	626	0.4	0.23[b]	18.4	5.7	-

[a] 1cSt = 1centistokes = 0.01cm²/s = 0.000001m²/s; [b] Yamashita and Iguchi (2003); [c] measured values.

Slag, steel and argon properties set to model are listed in Table 2. The standard operational prototype gas flow rate was considered (140 Nm³/h).

Table 2 – Physical properties set on RH numerical model.

	steel	argon	slag
Density (kg m^{-3})	7000	1.623	3500[(a)]
Temperature (°C)	1600	25	1600
Dynamic viscosity (mPa.s)	5.7	0.04848	100[(a)]
Interfacial tension (N m^{-1})	steel/argon		steel/slag
	=> 1.54		=> 1.5[(b)]

[(a)] Kang *et al.* (2003); [(b)] Nakashima and Mori (1992)

2.3 Desulfurization kinetic model

From the results obtained in physical and numerical modeling, a kinetic model has been developed to predict sulfur removal by desulfurizer reagent addition into the vacuum chamber. This model consists of a numerical solution for the adapted Deo and Boom (1993) desulfurization model (Peixoto, 2019), as schematized in Figure 2.

In the model, the following considerations were taken into account:

• The holding time (t_H) of slag in the vacuum chamber was determined for two gas flow rates based on physical modeling using N-pentane to emulate slag, see (Peixoto, 2019);

• The residence time (t_{RP}), for each droplet group (fraction) size, has been defined using Particle Transport Model, implemented in ANSYS-CFX;

• The mass transfer coefficient (El-Kaddah and Szekely (1981) model) was calculated taking into consideration all diameters set in ANSYS-CFX and ε (average value in the ladle) from this software, for both gas flow rates, 90 and 140 Nm³/h;

• The W parameter, related to the number of droplets drawn to the ladle, was calculated according to the slag mass fraction for each size fraction and given holding time.

The de-S kinetic model was solved for all particle size groups, and their corresponding parameters. The sum of individual desulfurization contribution, related to each particle size fraction, gives the total S removal degree.

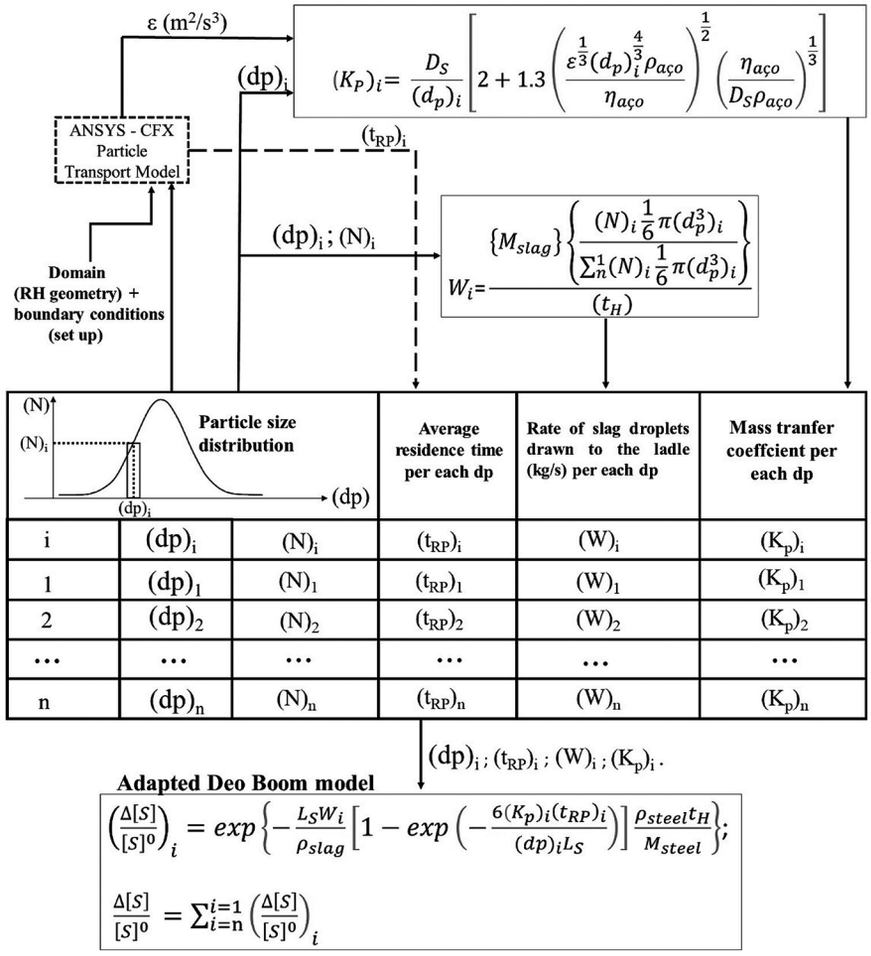

Figure 2 - Schematics of numerical calculation of de-S at RH degasser.

The Sulfur partition coefficient was calculated from the following relationships, Equations (4) and (5), available in literature (Slag Atlas).

$$\log L_s = \frac{21920 - 54640\lambda_0}{T} + 43.6\lambda_0 - 23.9 - \log(\%O) \quad (4)$$

$$\log \frac{h_{Al}^2 h_O^3}{a_{Al_2O_3}} = \frac{-64000}{T} + 20.57 \quad (5)$$

Here: λ_0 is the slag optical basicity; T is the temperature (K); h_i is the activity of the specie i; (%O) is the oxygen steel content and a_{Al2O3} is alumina activity in the slag phase.

3. Results and discussion

3.1 Droplets dispersion inside RH - numerical and physical models

The circulation rate estimated by the herein described numerical procedure is in accordance with the Kuwabara equation, see previous article by Peixoto *et al.* (2018), which is a good indicator for a similar flow pattern in the prototype and models. Moreover, the oil added in the vacuum chamber is dragged to the ladle and virtually all oil is floated to the top layer.

Figure 3 depicts a sequence of images illustrating how oil density influences the droplet dispersion. High density soybean oil, close to water density, presents large droplet dispersion and it recirculates between the vacuum chamber and ladle. In the case of N-Pentane, the density difference is larger, so the droplet flow is restricted to the region near the down-leg jet, without recirculation. In the case of 10W30 engine oil, of intermediary density, it presents intermediary behavior too. Moreover, it is possible to see gas flow rate influence on reagent dispersion in the lower vessel. These observations are valid for physical and numerical modeling, providing similarity is kept.

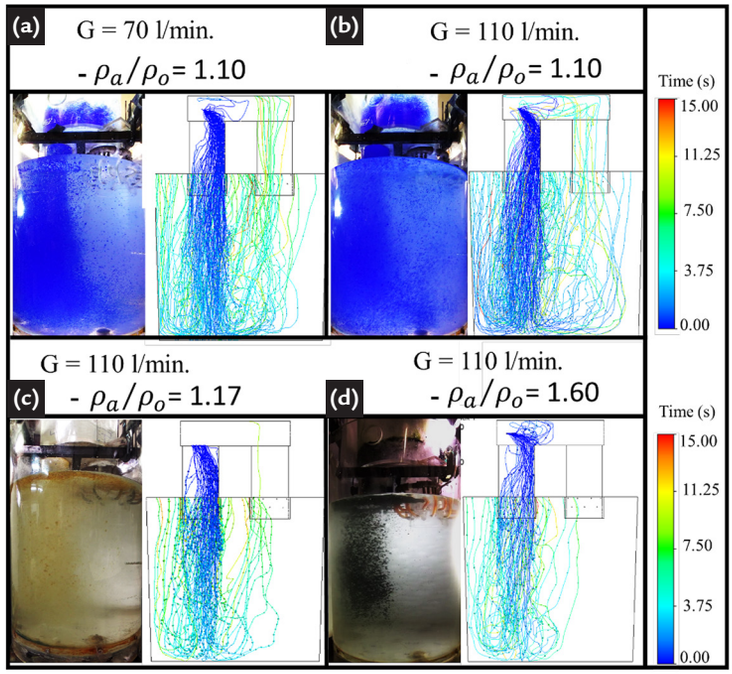

Figure 3 - Oil droplets behavior assessed by numerical and physical modeling for different phases density ratio: soybean oil (a) 70 l/min and (b) 110 l/min; (c) 10W30 engine oil and (d) N-pentane oil.

In regard to the analysis of droplet size influence on its motion inside RH degasser, three particle sizes were considered: 10, 7 and 5 mm. As in the case with N-Pentane, it is observed (Figure 4) that the slag droplet flow is restricted to regions below and around the down leg, mainly due to buoyancy effects, especially for coarse drop size (10 mm).

Another important parameter in regard to dispersed phase behavior is the residence time, herein taken as the time required for slag droplets to reach the top ladle layer (free board in the numerical modeling). From the physical model, the average residence times were 43 s, 70 s and 100 s, approximately, for the particle sizes of: 10 mm, 8 mm and 7 mm, respectively (lower half of time scale).

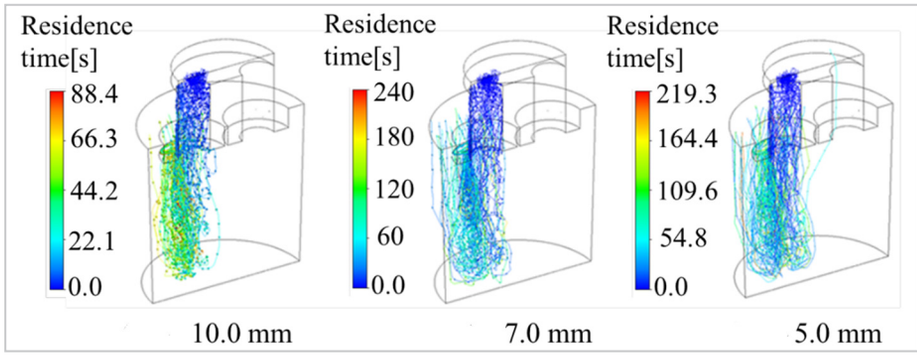

Figure 4 - Influence of slag drop size in its residence time dispersed into molten steel.

Physical modeling experiments using N-pentane/water combination almost faithfully describe slag-steel behavior in RH obtained from CFX, confirming that difference in phases density is the most important parameter that influences droplet trajectories and residence time inside steel.

Numerical (ANSYS-CFX) model has been validated, by physical model experiments, to simulate continuous phase flow pattern and second phase behavior (droplets trajectory and residence time), even for a large density difference. Therefore, the numerical model here developed is useful to predict slag droplet-steel behavior.

3.2 Mass transfer analysis

Figure 5 presents the case in which 10W30 engine oil was used: low refining efficiency, around 4%, is obtained at the RH model. This is explained by the lower thymol partition coefficient for this oil. As can be seen, the thymol extraction was more expressive in the bench experiments, where oil dispersion is sustained by stirring, which is not the case for the RH cold model.

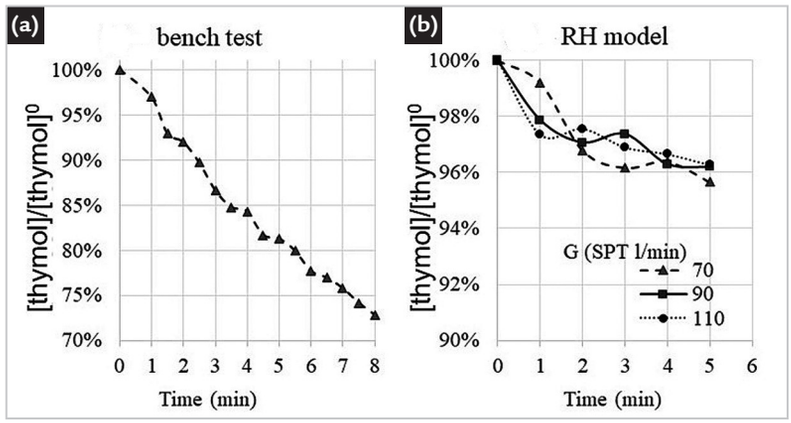

Figure 5 - Mass transfer experiments with 10W30 engine oil. (a) –beaker experiments, (b) –RH physical model experiments. [thymol] stands for thymol aqueous solution concentration.

With soybean oil, which has high L_t (~400), thymol extraction ranges from 15% to 25%, for different oil injection times and gas flow rates, as can be seen in Figure 6. It is observed that shorter oil addition times result in oscillation of thymol concentration values (Figure 6-(a) and (b)), probably due to the mixing time in the ladle, since there is a certain periodicity in peak concentration. This behavior has been observed for the two duplicate tests. This oscillation was not observed for oil injection time equal to 85 s, see Figure 6-(c). In all cases, the concentration of thymol strongly decreases during the first four minutes, approximately. Thymol removal after four minutes occurs for all injection times due to small droplet recirculation, caused by the low water - oil density difference.

With circulation rates increasing, caused by an increase of the gas flow rate, the residence time for dispersed oil droplets is larger, which is beneficial to impurity removal in the cold model. A high circulation rate reduces the buoyancy effect on oil droplets, since the recirculatory flow is more intense.

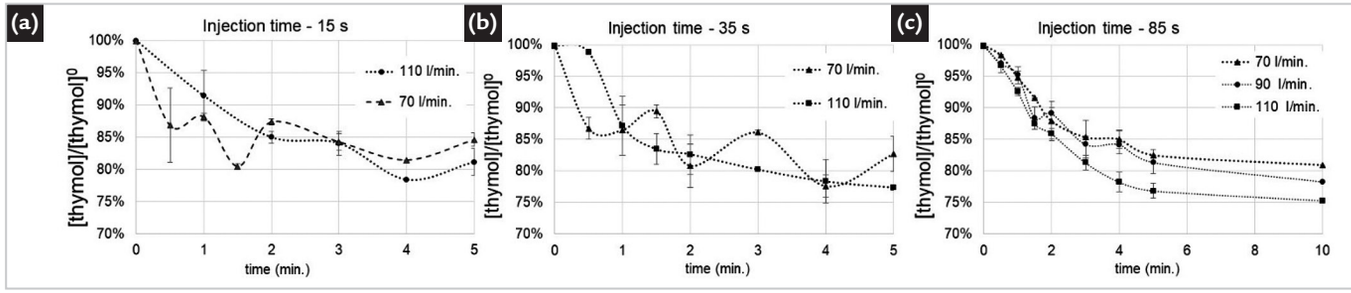

Figure 6 - Relative changes of thymol aqueous solution concentration ([thymol]) as a function of time, injection time and gas flow rate.

Oil droplet recirculation between the vacuum chamber and ladle can be observed in Figure 7. As can be seen, small oil drops remain dispersed inside the continuous phase 5 minutes after the injection ends. After 60 s, a thicker oil layer has been formed as a ladle top layer; however it is difficult to make an estimation of the small oil fraction in recirculation. Even though the amount of this oil in recirculation is small, its effect on thymol extraction is significant, since it has a high interfacial area. However, droplet recirculation is not expected in the prototype due to the high density difference between slag and steel, as shown before. Thus, desulphurization increases due to the increasing circulation rate are not expected in the prototype, as will be demonstrated in the next topic.

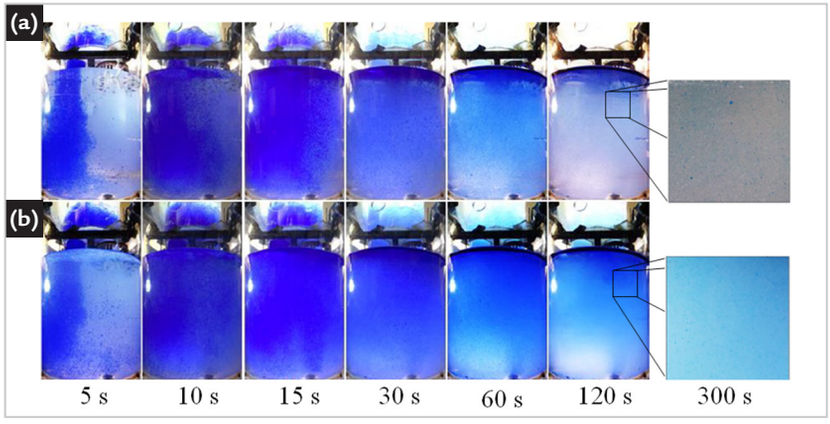

Figure 7 - Influence of gas flow rate in oil droplet dispersion and recirculation.

3.3 Steel desulfurization

Results from the kinetic model for steel desulfurization, considering gas flow rates of 90 Nm^3/h and 140 Nm^3/h, are presented in Figure 8. It can be observed that after 135 and 235 s, for the gas flow rate of 140 and 90 Nm^3/h, respectively, no further desulfurization occurs, as the desulfurizer agent is incorporated into the ladle stagnant slag, which is inactive for desulfurization (Silva *et al.*, 2021). At the final stage on RH (tf) the de-S degree ranges from 19.50 to 31.44%, which is in agreement with the results from industrial trials provided by Zhan *et al.* (2006), Silva *et al.* (2015), Yang *et al.* (2014) and He *et al.* (2012). The overall operational conditions mentioned by these authors are comparable to the ones taken in account for the kinetic model developed in this study. That is, basic slag ($CaO-Al_2O_3-CaF_2-MgO-SiO_2$) added in the range from 5 to 10 kg/ton. Moreover, they are applied to a steel with low oxygen content, which is very common to RH treatment.

Even though the de-S rate (d%S/dt; removal rate) is a bit larger for 140 Nm^3/h, the final sulfur content in steel is lower when the lower gas flow rate is set. The key parameter concerning RH desulfurization by reagent addition into vacuum chamber is the slag droplet residence time into steel, and residence time increases as the gas flow rate (circulation rate) is reduced.

The de-S refining step is short when compared with the total degassing time. Then, for desulfurization purposes, it is worth reducing the gas flow rate before desulfurizer reagent addition, resuming standard gas flow rate afterwards. Therefore, with this gas flow rate management, a satisfactory S removal can be achieved without reduction in productivity or even increase of heat losses.

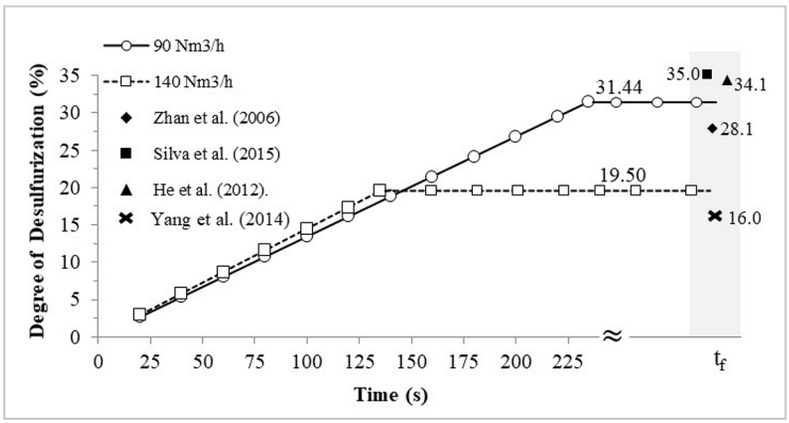

Figure 8 - Degree of desulfurization as a function of time for two gas flow rates.

The industrial RH desulfurization trials performed by Silva *et al.* (2015) have been done under conditions very close to those taken into account to develop this kinetic model, as slag amount (10 kg/ton). As can be seen in Figure 9, there is a good agreement between final S content provided (measured) by Silva *et al.* (2015) and values calculated by the present model (taking into account the initial steel sulfur content reported by these authors in their tests).

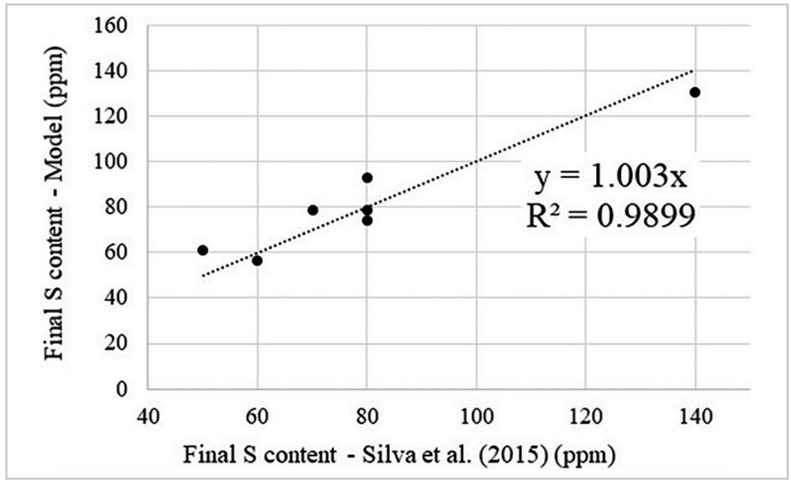

Figure 9 – Final sulfur content: kinetic model prediction versus industrial data.

RH is typically the last opportunity for sulfur removal. Therefore, for common steels grades, this desulfurization technique is useful too, since moderate corrections in heat that eventually leaves the sulfur content higher than the required one, can be done. This implies that reprocessing or even additional processing, which could lead to a loss of sequence in the steelmaking route, will not be necessary, since the de-S on RH is a quick reaction.

4. Conclusions

The main parameter regarding oil droplet behavior in a RH cold model is density difference. As it increases, the restriction on droplet flow increases too. From the mass transfer experiments on a cold model, it was observed that the refining efficiency is high for high injection time and high gas flow rate, since oil droplet recirculation is significant in this case, due to the low-density difference between the continuous and dispersed phases. As far as the prototype is concerned, as the slag-steel density difference is larger, the simulation showed a different behavior, in which de-S is reduced as the circulation rate increases. The desulfurization model in the RH degasser suggests a good performance for this operation, as steel composition adjustments can be done without compromising steel productivity. Moreover, for ultra-low sulfur steel production, it is an interesting technique. For desulfurization purposes, it is worth reducing the gas flow rate before the desulfurizer reagent addition, resuming standard gas flow rate afterwards, since the dispersed phase residence time seems to control the total of Sulphur removed.

References

ABREU, S. G. P. T.; OLIVEIRA, T. A. S.; ANANIAS, J. V. G. G.; QUEIROZ, G. S.; SILVA, I. A.; SILVA, C. A.; PEIXOTO, J. J. M. Modelamento físico de transferência de massa aplicado ao refino do aço. *In*: SEMINÁRIO DE ACIARIA, FUNDIÇÃO E METALURGIA DE NÃO-FERROSOS, 50, 2019, São Paulo. ***Anais [...].*** São Paulo: ABM, 2019. p. 638–648.

ALLIBERT, M. *et al*. ***Slag atlas***. Düsseldorf: Verlag Stahleisen Gmbh. 1995. 634p.

ANSYS. ***ANSYS CFX- Solver theory guide.*** Release 18.2. Canonsburg, PA: Ansys. Inc., 2017. 366p.

DAI, W.; CHENG, G.; ZHANG, G.; HUO, Z.; LV, P.; QIU, Y.; ZHU, W. Investigation of circulation flow and slag-metal behavior in an industrial Single Snorkel Refining Furnace (SSRF): application to desulfurization. Metallurgical and Materials Transactions B: Process ***Metallurgy and Materials Processing Science***, v. 51, n. 2, p. 611–627, 2020.

DEO, B.; BOOM, R. ***Fundamentals of steelmaking metallurgy.*** London: Prentice Hall International, 1993. 300p.

EL-KADDAH, N.; SZEKELY, J. Mathematical model for desulphurization kinetics in argon-stirred ladles. ***Ironmaking and Steelmaking,*** v. 8, n. 6, p. 269–278, 1981.

GHOSH, A. ***Secondary steelmaking:*** principles and applications. New York: CRC Press LLC, 2001. 308p.

HE, S.; ZHANG, G.; WANG, Q. Desulphurisation process in RH degasser for soft-killed ultralow-carbon electrical steels. ***ISIJ International,*** v. 52, n. 6, p. 977–983, 2012.

KANG, S. M.; KIM, D. Y.; KIM, J. S.; LEE, H. G. Sulfur transfer in dynamic conditions of liquid steel drops falling through slag layer. ***ISIJ International,*** v. 43, n. 11, p. 1683–1690, 2003.

NAKASHIMA, K.; MORI, K. Interfacial properties of liquid iron alloys and liquid slags relating to iron- and steel-making processes. ***ISIJ International***, v. 32, n. 1, p. 11–18, 1992.

RIBOUD, P.; VASSE, R. Désulfuration de l'acier en poche-synthèse des résultats théoriques et industriels. ***Revue de Métallurgie - CIT,*** v. 82, n. 11, p. 801–810, 1985.

PEIXOTO, J. J. M. ***Análise da turbulência e do comportamento metal-escória no interior de um reator RH e sua influência sobre a reação de dessulfuração do aço.*** 2019. 205 f. Tese (Doutorado em Engenharia de Materiais) –

REDEMAT, Escola de Minas, Universidade Federal de Ouro Preto, Ouro Preto, 2019.

PEIXOTO, J. J. M.; GABRIEL, W. V.; OLIVEIRA, T. A. S.; SILVA, C. A.; SILVA, I. A.; SESHADRI, V. Numerical simulation of recirculating flow and physical model of slag–metal behavior in an RH Reactor: application to desulfurization. ***Metallurgical and Materials Transactions B***: Process Metallurgy and Materials Processing Science, v. 49, n. 5, p. 2421–2434, 2018.

SESHADRI, V.; COSTA, S. L. S. Cold model studies of R. H. Degassing Process. ***ISIJ International,*** v. 26, n. 2, p. 133–138, 1986.

SILVA, A. M. B.; OLIVEIRA, M. A.; PEIXOTO, J. J. M.; SILVA, C. A. Slag-steel emulsification on a modified RH degasser. ***Metallurgical and Materials Transactions B:*** Process Metallurgy and Materials Processing Science, v. 52, p. 2111-2126, 2021.

SILVA, T. C.; RODRIGUES, E. F.; SOARES, C.; SILVA, C. A.; SILVA, I. A. Simulação numérica do fluxo recirculatório em um reator RH: aplicação à dessulfuração. *In:* SEMINÁRIO DE ACIARIA, FUNDIÇÃO E METALURGIA DE NÃO-FERROSOS, 46., 2015, Rio de Janeiro. ***Anais [...].*** Rio de Janeiro: ABM, 2015. p. 194–203.

TORRES, F. M. ***Modelamento físico e matemático dos efeitos da injeção auxiliar de gás em um reator Kanbara.*** 2017. 65 f. Dissertação (Mestrado em Engenharia de Materiais) – REDEMAT, Escola de Minas, Universidade Federal de Ouro Preto, Ouro Preto, 2017.

VAN DER KNOOP, W; TIEKINK, W.; DE JONG, V. P. Desulphurisation during RH treatment at Hoogovens Staal. ***Revue de Metallurgie-CIT***, v. 93, n. 4, p. 533–540, 1996.

WEI, J. H.; ZHU, S. J.; YU, N. W. Kinetic model of desulphurization by powder injection and blowing in RH refining of molten steel. ***Ironmaking and Steelmaking,*** v. 27, n. 2, p. 129–137, 2000.

YAMASHITA, S.; IGUCHI, M. Control of reverse emulsification and mixing time in a bottom blown bath covered with top slag. ***ISIJ International,*** v. 43, n. 9, p. 1326–1332, 2003.

YANG, H.; YANG, S.; LI, J.; ZHANG, J. A mathematical model to characterize RH desulfurization process. ***Journal of Iron and Steel Research International,*** v. 21, n. 11, p. 995–1001, 2014.

ZHAN, D. P.; JIANG, Z. H.; WANG, W. Z. Development of deep desulfurization technology with premelted slag during RH-KTB refining. ***Developments in Chemical Engineering and Mineral Processing,*** v. 14, n. 3/4, p. 375–384, 2006.

ZULHAN, Z.; SCHRADE, C.; PATRIONA, Y. A. Desulphurization of molten steel in RH-Degasser by powder blowing to produce Non-Grain Oriented (NGO) silicon steel. ***SEAISI Quarterly Journal,*** v. 42, n. 4, p. 32–36, 2013.

Received: 5 August 2021 - Accepted: 2 November 2021.